

Activation function dependence of the storage capacity of treelike neural networks

Jacob A. Zavatone-Veth*

Department of Physics, Harvard University, Cambridge, Massachusetts 02138, USA

Cengiz Pehlevan†

John A. Paulson School of Engineering and Applied Sciences,
Harvard University, Cambridge, Massachusetts 02138, USA and

Center for Brain Science, Harvard University, Cambridge, Massachusetts 02138, USA

(Dated: June 10, 2022)

The expressive power of artificial neural networks crucially depends on the nonlinearity of their activation functions. Though a wide variety of nonlinear activation functions have been proposed for use in artificial neural networks, a detailed understanding of their role in determining the expressive power of a network has not emerged. Here, we study how activation functions affect the storage capacity of treelike two-layer networks. We relate the boundedness or divergence of the capacity in this limit to the smoothness of the activation function, elucidating the relationship between previously studied special cases. Our results show that nonlinearity can both increase capacity and decrease the robustness of classification, and provide simple estimates for the capacity of networks with several commonly used activation functions.

The expressive power of artificial neural networks is well-known [1–4], but a complete theoretical account of how their remarkable abilities arise is lacking [5, 6]. In particular, though a diverse array of nonlinear activation functions have been employed in neural networks [5–12], our understanding of the relationship between choice of activation function and computational capability is incomplete [7–9]. Methods from the statistical mechanics of disordered systems have enabled the interrogation of this link in several special cases [9–15], but these previous works have not yielded a general theory.

In this work, we characterize how pattern storage capacity depends on activation function in a tractable two-layer network model known as the treelike committee machine. We find that the storage capacity of a treelike committee machine remains finite in the infinite-width limit provided that the activation function is weakly differentiable, and it and its weak derivative are square-integrable with respect to Gaussian measure. For example, the capacity with sign activation functions diverges, while that with rectified linear unit or error function activations is finite. We predict that nonlinearity should increase capacity, but may reduce the robustness of classification. These connections between expressive power and smoothness begin to shed light on the influence of activation functions on the capabilities of neural networks.

The treelike committee machine—The treelike committee machine is a two-layer neural network with N inputs divided among K hidden units into disjoint groups of N/K and binary outputs (Figure 1a) [9–12]. For a hidden unit activation function g , a set of hidden unit weight vectors $\{\mathbf{w}_j \in \mathbb{R}^{N/K}\}_{j=1}^K$, a readout weight vector $\mathbf{v} \in \mathbb{R}^K$,

and a threshold $\vartheta \in \mathbb{R}$, its output is given as

$$y(\mathbf{x}) = \text{sign}(s(\mathbf{x})) \quad \text{for} \quad (1)$$

$$s(\mathbf{x}; \{\mathbf{w}_j\}, \mathbf{v}, \vartheta) = \frac{1}{\sqrt{K}} \sum_{j=1}^K v_j g \left(\frac{\mathbf{w}_j \cdot \mathbf{x}_j}{\sqrt{N/K}} \right) - \vartheta, \quad (2)$$

where \mathbf{x}_j denotes the vector of inputs to the j^{th} hidden unit. In this model, the readout weight vector and threshold are fixed, and only the hidden unit weights are learned. The perceptron can thus be viewed as the special case of a treelike committee machine with identity activation functions and equal readout weights [13, 14].

Statistical mechanics of pattern storage—To characterize this network’s ability to classify a random dataset of P examples subject to constraints on the hidden unit weights imposed by a measure ρ , we define the Gardner

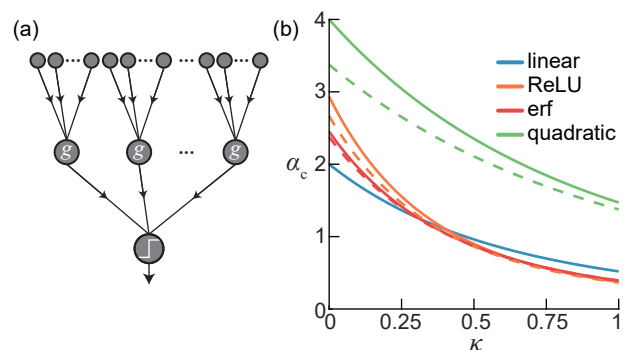


FIG. 1. Pattern storage in treelike committee machines. (a) Network architecture. (b) Capacity α_c as a function of margin κ for several common activation functions. Solid and dashed lines indicate estimates of the capacity under replica-symmetric and one-step replica-symmetry-breaking ansätze, respectively.

* jzavatoneveth@g.harvard.edu

† cpehlevan@seas.harvard.edu

volume [13, 14]

$$Z = \int d\rho(\{\mathbf{w}_j\}) \prod_{\mu=1}^P \Theta(y^\mu s(\mathbf{x}^\mu; \{\mathbf{w}_j\}, \mathbf{v}, \vartheta) - \kappa), \quad (3)$$

which measures the volume in weight space such that all examples are classified correctly with margin at least κ . As in most studies of the Gardner volume of neural networks, we consider a dataset consisting of Bernoulli disorder, in which the components of the inputs and the target outputs are independently and identically distributed as $x_{jk}^\mu = \pm 1$ and $y^\mu = \pm 1$ with equal probability [9–15]. We consider “spherical” committee machines, in which the hidden unit weight vectors lie on the sphere of radius $(N/K)^{1/2}$ [9–11, 13].

We will study the sequential infinite-width limit $N, P \rightarrow \infty$, $K \rightarrow \infty$, with load $\alpha \equiv N/P = \mathcal{O}(1)$. In this limit, we expect the free entropy per weight $f = N^{-1} \log Z$ to be self-averaging with respect to the distribution of the quenched disorder [12], and for there to exist a critical load α_c , termed the capacity, below which the classification task is solvable with probability one and above which Z vanishes [12–15]. The special case of this model with sign activation functions was intensively studied in the late 20th century, showing that the capacity diverges as $K \rightarrow \infty$ [10, 11, 16]. In contrast, Baldassi *et al.* [9] recently showed that the capacity with rectified linear unit (ReLU) activations remains bounded in the infinite-width limit. Our primary objective in this work is to identify the class of activation functions for which the capacity remains finite.

We begin our analysis by specifying our choice of general constraints on the activation function, readout weights, and threshold. We will require the $K \rightarrow \infty$ limit to be well-defined in the sense that the variance of the output preactivation s over the pattern distribution is finite. In the sequential limit, the central limit theorem implies that hidden unit preactivations converge in distribution to a collection of independent Gaussian random variables [17]. Therefore, for s to have finite variance, the activation function g must lie in the Lebesgue space $\mathcal{L}^2(\gamma)$ of functions that are square-integrable with respect to the Gaussian measure γ on the reals (see Appendix A). Furthermore, as $\text{var}(s) \propto \|\mathbf{v}\|_2^2/K$, we must have $\|\mathbf{v}\|_2 = \mathcal{O}(\sqrt{K})$. Observing that $\|\mathbf{v}\|_2$ sets the effective scale of ϑ and κ but does not affect the zero-margin capacity, we fix $\|\mathbf{v}\|_2 = \sqrt{K}$ for convenience. To ensure that s has mean zero, we set $\vartheta = K^{-1/2}(\mathbb{E}g) \sum_{j=1}^K v_j$, where $\mathbb{E}g = \int d\gamma(z) g(z)$ is the average value of the hidden unit activations. This choice maximizes the capacity for the symmetric datasets of interest (see Appendices B, C, and D), and generalizes the conditions on \mathbf{v} and ϑ considered in previous works [9–11].

To compute the limiting quenched free entropy, we apply the replica trick, which exploits a limit identity for logarithmic averages and a non-rigorous interchange of

limits to write

$$f = \lim_{n \downarrow 0} \lim_{K \rightarrow \infty} \lim_{N \rightarrow \infty} \frac{1}{nN} \log \mathbb{E}_{\mathbf{x}, y} Z_{N, \alpha, N, K}^n, \quad (4)$$

where the validity of analytic continuation of the moments from positive integer n to $n \downarrow 0$ is assumed [13, 15, 18]. This calculation is standard, and we defer the details to Appendix B.

In this limit, the quenched free entropy can be expressed using the method of steepest descent as an extremization over the Edwards-Anderson order parameters $q_j^{ab} = (K/N) \mathbf{w}_j^a \cdot \mathbf{w}_j^b$ [13, 15, 18], which represent the average overlap between the preactivations of the j^{th} hidden unit in two different replicas a and b . Under a replica- and hidden-unit-symmetric (RS) ansatz $q_j^{ab} = q$, one finds that

$$f_{\text{RS}} = \text{extr}_q \left\{ \alpha \int d\gamma(z) \log H \left(\frac{\kappa + \sqrt{\tilde{q}(q)} z}{\sqrt{\sigma^2 - \tilde{q}(q)}} \right) + \frac{1}{2} \left[\frac{1}{1-q} + \log(1-q) + \log(2\pi) \right] \right\}, \quad (5)$$

where $H(z) = \int_z^\infty d\gamma(x)$ is the Gaussian tail distribution function, $\sigma^2 = \mathbb{E}g^2 - (\mathbb{E}g)^2$ is the variance of the activation, and

$$\tilde{q}(q) = \text{cov} \left[g(x), g(y); \begin{bmatrix} x \\ y \end{bmatrix} \sim \mathcal{N} \left(0, \begin{bmatrix} 1 & q \\ q & 1 \end{bmatrix} \right) \right] \quad (6)$$

is an effective order parameter describing the average overlap between the activations of a given hidden unit in two different replicas. This expression for f_{RS} is equivalent to that given in [9] for ReLU activations, but we adopt a different definition for the effective order parameter that has a clearer statistical interpretation for generic activation functions.

To find the replica-symmetric capacity α_{RS} , one must take the limit $q \uparrow 1$ in the saddle point equation that defines the extremum with respect to q , as the Gardner volume tends to zero in this limit [9–14]. As $q \uparrow 1$, $\tilde{q} \uparrow \sigma^2$, but the asymptotic properties of \tilde{q} as a function of $\varepsilon \equiv 1 - q$ depend on the choice of activation function. Making the general ansatz that $\sigma^2 - \tilde{q} \sim \varepsilon^\ell$ for some $\ell > 0$, we find that $\alpha_{\text{RS}} \sim \varepsilon^{\ell-1}$ (see Appendix C). Therefore, the RS capacity diverges if $\ell < 1$ and vanishes if $\ell > 1$, while the boundary case $\ell = 1$ is special in that the capacity is bounded but non-vanishing. For the special cases of $g(x) = \text{sign}(x)$ and $g(x) = \text{ReLU}(x)$, this behavior was noted by Baldassi *et al.* [9]. For sign, one has $\sigma^2 - \tilde{q} \sim \sqrt{\varepsilon}$, and α_{RS} diverges in the infinite-width limit, while for ReLU, $\sigma^2 - \tilde{q} \sim \varepsilon$, and α_{RS} remains finite. However, [9] and other previous studies [10, 11] relied on direct computation of the effective order parameters for all values of q , which is not tractable for most activation functions, and does not yield general insight.

Asymptotics of the effective order parameter—To understand the asymptotic behavior of $\tilde{q}(q)$ as $q \uparrow 1$ for general activation functions g , we apply tools from the

theory of Gaussian measures [19]. As g is in $\mathcal{L}^2(\gamma)$ by assumption, it has a Fourier-Hermite series

$$g(x) = \sum_{k=0}^{\infty} g_k \text{He}_k(x), \quad (7)$$

where $\{\text{He}_k\}$ is the set of orthonormal Hermite polynomials (see Appendix A). We note that the $\mathcal{L}^2(\gamma)$ norm of g can then be written as the sum of the squares of the coefficients g_k , i.e. $\|g\|_{\gamma}^2 = \sum_{k=0}^{\infty} g_k^2$, and that $g_0 = \mathbb{E}g$. To express $\tilde{q}(q)$ in terms of these coefficients, we recall the Mehler expansion of the standard bivariate Gaussian density $\varphi(x, y; q)$ [20, 21]:

$$\varphi(x, y; q) = \varphi(x)\varphi(y) \sum_{k=0}^{\infty} q^k \text{He}_k(x) \text{He}_k(y), \quad (8)$$

where $\varphi(x) = \exp(-x^2/2)/\sqrt{2\pi}$ is the univariate Gaussian density. Then, we can evaluate the expectation in (6), yielding

$$\tilde{q}(q) + g_0^2 = \sum_{k=0}^{\infty} g_k^2 q^k, \quad (9)$$

which, by Abel's theorem, is a bounded, continuous function of $q \in [-1, 1]$ because $\tilde{q}(1) + g_0^2 = \|g\|_{\gamma}^2$ is finite. Writing $q \equiv 1 - \varepsilon$, we expand $(1 - \varepsilon)^k$ in a binomial series and formally interchange the order of summation to obtain

$$\tilde{q}(\varepsilon) + g_0^2 = \sum_{l=0}^{\infty} \frac{(-\varepsilon)^l}{l!} \sum_{k=l}^{\infty} (k)_l g_k^2, \quad (10)$$

where $(k)_l = k(k-1)\cdots(k-l+1)$ is the falling factorial. We recognize the sums over k as the norms of the weak derivatives of g , which have formal Fourier-Hermite series

$$g^{(l)}(x) = \sum_{k=l}^{\infty} g_k \sqrt{(k)_l} \text{He}_{k-l}(x), \quad (11)$$

which follow from the recurrence relation $\text{He}'_k(x) = \sqrt{k} \text{He}_{k-1}(x)$ [19]. Therefore, \tilde{q} admits a formal power series expansion in ε as

$$\tilde{q}(\varepsilon) + g_0^2 = \sum_{l=0}^{\infty} \frac{(-1)^l}{l!} \|g^{(l)}\|_{\gamma}^2 \varepsilon^l. \quad (12)$$

For the RS capacity to remain bounded, we merely require that the first two terms in this series are finite, not for the series to converge at any higher order for non-vanishing ε . Therefore, the RS capacity is finite for once weakly-differentiable activations g such that the \mathcal{L}^2 norms of the function and its weak derivative with respect to Gaussian measure, $\|g\|_{\gamma}$ and $\|g'\|_{\gamma}$, are finite. This class of functions is precisely the Sobolev class $\mathcal{H}^1(\gamma)$ [19]. We provide additional background material on $\mathcal{H}^1(\gamma)$ and weak differentiability in Appendix A.

Storage capacity—For any activation function in the class $\mathcal{H}^1(\gamma)$, we find that

$$\alpha_{\text{RS}}(\kappa) = \frac{\|g'\|_{\gamma}^2}{\sigma^2} \alpha_{\text{G}}\left(\frac{\kappa}{\sigma}\right), \quad (13)$$

where

$$\alpha_{\text{G}}(\kappa) = \left[\int_{-\kappa}^{\infty} d\gamma(z) (\kappa + z)^2 \right]^{-1} \quad (14)$$

is Gardner's formula for the perceptron capacity [13] (see Appendix C). In terms of Fourier-Hermite coefficients, we have $\sigma^2 = \sum_{k=1}^{\infty} g_k^2$ and $\|g'\|_{\gamma}^2 = \sum_{k=1}^{\infty} k g_k^2$. Thus, we have $\|g'\|_{\gamma}^2 \geq \sigma^2$, with equality if and only if all nonlinear terms (those corresponding to Hermite polynomials of degree two or greater) vanish. Therefore, introducing nonlinearity always increases the zero-margin RS capacity. However, as $\alpha_{\text{G}}(\kappa)$ is a monotonically decreasing function, the capacity at large margins can be reduced by nonlinearity if $\sigma < 1$. We note that the zero-margin capacity is invariant under rescaling of the activation function and hidden unit weights as $g \mapsto c_1 g$, $\mathbf{v} \mapsto c_2 \mathbf{v}$ for some constants c_1 and c_2 . For finite margin, rescaling can increase or decrease the capacity by changing σ . Thus, in the sense of classification margin, introducing nonlinearity or re-scaling can reduce the robustness of classification.

Using this result, we can characterize the RS capacity of wide treelike committee machines for several commonly-used activation functions (see Appendix E for details). As previously noted, for a linear activation function, our result reduces to Gardner's perceptron capacity [13]. As the sign function is not weakly differentiable, we recover the result that the capacity diverges [10, 11]. ReLU is weakly differentiable, and we recover the result from [9] that $\alpha_{\text{RS}} = 2\pi/(\pi - 1) \simeq 2.93388$. Considering sigmoidal activations, we find that $\alpha_{\text{RS}} = 2 \arcsin(2/3)/\pi \simeq 2.45140$ for the error function, while $\alpha_{\text{RS}} \simeq 2.35561$ for the hyperbolic tangent and the logistic function. As an example of a non-monotonic activation function, we consider a quadratic, which yields $\alpha_{\text{RS}} = 4$. We plot the RS capacity as a function of margin for these activation functions in Figure 1b, illustrating how nonlinearity can reduce the large-margin capacity.

To demonstrate the applicability of our theory to more exotic activation functions, we consider several smooth, non-monotonic alternatives to ReLU that have been proposed in the deep learning literature [7, 8]. All of these functions are in $\mathcal{H}^1(\gamma)$, hence they yield finite capacities, which we estimate in Appendix E. In summary, our replica-symmetric calculation divides activation functions into those that are outside $\mathcal{H}^1(\gamma)$, for which the capacity diverges, and those that are in $\mathcal{H}^1(\gamma)$, for which the capacity is finite and given by (13). For functions in $\mathcal{H}^1(\gamma)$, our RS result predicts that nonlinearity should increase capacity, but can decrease classification robustness.

However, for nonlinear activation functions, one generically expects the energy landscape to become locally

non-convex, and for replica symmetry breaking (RSB) to occur [9–12, 15, 18]. The RS estimate of the capacity is therefore only an upper bound, and one must account for RSB effects in order to obtain a more accurate estimate [9–12, 15, 16, 18]. To that end, we have calculated the capacity under a one-step replica-symmetry-breaking (1-RSB) ansatz, extending the results of earlier work [9–11] to arbitrary activation functions. Under the 1-RSB ansatz, the replicas are divided into groups of size m , with inter-group overlap q_0 and intra-group overlap q_1 . Then, the capacity is extracted by taking the limit $q_1 \uparrow 1$, $m \downarrow 0$, with $r \equiv m/(1 - q_1)$ finite [9–12, 18].

As detailed in Appendix D, this calculation yields an expression for $\alpha_{1\text{-RSB}}$ as the solution to a two-dimensional minimization problem over q_0 and r . Importantly, the finite-capacity condition at 1-RSB is the same as that with RS. For functions in $\mathcal{H}^1(\gamma)$, the resulting minimization problem must usually be solved numerically, hence we give results for only a few tractable examples. For these examples, we illustrate this minimization problem by plotting its landscape in Figure 2. For comparison purposes, we include the landscape for linear activation functions, for which RSB does not occur [13–15, 22]. For ReLU, we obtain $\alpha_{1\text{-RSB}} \simeq 2.66428$ at $(q_0^*, r^*) \simeq (0.75716, 16.6374)$. This result is slightly lower than the $\alpha_{1\text{-RSB}} \simeq 2.92$ reported by [9], a discrepancy which likely results from differences in numerical analysis (see Appendix E). For erf, we obtain $\alpha_{1\text{-RSB}} \simeq 2.37500$ at $(q_0^*, r^*) \simeq (0.75463, 7.75682)$. Finally, for the quadratic, we have $\alpha_{1\text{-RSB}}(\kappa = 0) \simeq 3.37466$ at $(q_0^*, r^*) \simeq (0.28452, 6.39299)$. In Figure 1, we plot the 1-RSB capacity for these activation functions at nonzero margins. The gap between the RS and 1-RSB results for the quadratic is larger than that for erf or ReLU, both in the numerical value of the capacity and in the difference between the inter- and intra-group overlaps. Though the capacities at 1-RSB are reduced relative to the RS result, their ordering for these activation functions is preserved.

Discussion—We have shown that the storage capacity of treelike committee machines with activation functions in $\mathcal{H}^1(\gamma)$ remains bounded in the infinite-width limit. Our results follow from a replica analysis of the Gardner volume, with the capacity given by a simple closed-form expression under a replica-symmetric ansatz and a two-dimensional minimization problem with one-step replica-symmetry-breaking. Depending on the activation function, a fully accurate determination of the capacity would likely require higher levels in the Parisi hierarchy of replica-symmetry-breaking ansätze [18]. Furthermore, it can be challenging to rigorously prove that the capacity results obtained using the replica method at any level of the Parisi hierarchy are correct [15, 18, 22–24]. With these caveats in mind, our results begin to elucidate how nonlinear activation functions affect the ability of neural networks ability to robustly solve classification problems.

The Gardner volume is agnostic to the choice of learning algorithm used to train the weights of the network, which makes it a general approach to studying storage

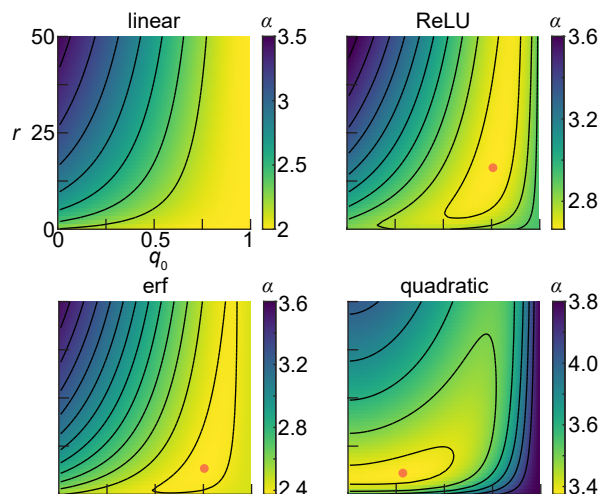


FIG. 2. The landscape of the function whose minimum determines the 1-RSB capacity as a function of the inter-block overlap q_0 and the rescaled Parisi parameter $r \equiv m/(1 - q_1)$ for several example activation functions. In each panel, the value of this function is shown in false color, with the location of minimum indicated by an orange dot.

capacity, but means that it can provide only limited insight into the practical realizability of the extant solutions [9–12]. In a recent study of least-squares function approximation by wide fully-connected committee machines, Panigrahi *et al.* [7] have shown using random matrix theory methods that the speed and robustness of learning with stochastic gradient descent is related to activation function smoothness. In particular, training error decreases rapidly with large decay exponent under weaker assumptions on the data for activation functions that have a “kink”—a jump discontinuity in their first or second derivatives—than for smooth functions. This result is suggestively similar to that of this work, as such functions are at most once or twice weakly-differentiable. However, further work will be required to determine whether a similar link between smoothness and trainability exists for classification tasks in treelike networks.

In this work, we have studied the activation-function-dependence of the storage capacity of wide treelike committee machines. This network architecture is particularly convenient to study in the infinite-width limit, but it is far removed from the deep networks used in practical applications [5]. As a step towards more elaborate and realistic models, one could consider a fully-connected committee machine, in which each hidden unit is connected to the full set of inputs. Prior work on such networks with sign activation functions suggests that some qualitative aspects of the behavior of treelike committee machines should still hold true [10, 11, 25]. However, fully-connected committee machines possess a permutation-symmetry with respect to interchange of the hidden units, which is broken at loads below the RS ca-

capacity [10]. This phenomenon and the presence of correlations between hidden units complicates the study of their infinite-width limit. Accurate determination of how their storage capacity depends on activation function will therefore require further work, in which the insights developed in this study should prove broadly useful.

Acknowledgements—J. A. Zavatone-Veth acknowledges support from the NSF-Simons Center for Mathematical and Statistical Analysis of Biology at Harvard and the Harvard Quantitative Biology Initiative. C. Pehlevan thanks the Harvard Data Science Initiative, Google, and Intel for support.

-
- [1] G. Cybenko, *Mathematics of control, signals and systems* **2**, 303 (1989).
- [2] K. Hornik, M. Stinchcombe, H. White, *et al.*, *Neural networks* **2**, 359 (1989).
- [3] C. Zhang, S. Bengio, M. Hardt, B. Recht, and O. Vinyals, in *5th Int. Conf. on Learning Representations (ICLR 2017)* (2016).
- [4] B. Poole, S. Lahiri, M. Raghu, J. Sohl-Dickstein, and S. Ganguli, in *Advances in neural information processing systems* (2016) pp. 3360–3368.
- [5] Y. LeCun, Y. Bengio, and G. Hinton, *Nature* **521**, 436 (2015).
- [6] I. Goodfellow, Y. Bengio, and A. Courville, *Deep learning* (MIT press, 2016).
- [7] A. Panigrahi, A. Shetty, and N. Goyal, arXiv preprint arXiv:1908.05660 (2019).
- [8] P. Ramachandran, B. Zoph, and Q. V. Le, arXiv preprint arXiv:1710.05941 (2017).
- [9] C. Baldassi, E. M. Malatesta, and R. Zecchina, *Physical Review Letters* **123**, 170602 (2019).
- [10] E. Barkai, D. Hansel, and H. Sompolinsky, *Physical Review A* **45**, 4146 (1992).
- [11] A. Engel, H. Köhler, F. Tschepke, H. Vollmayr, and A. Zippelius, *Physical Review A* **45**, 7590 (1992).
- [12] A. Engel and C. Van den Broeck, *Statistical mechanics of learning* (Cambridge University Press, 2001).
- [13] E. Gardner, *Journal of Physics A: Mathematical and General* **21**, 257 (1988).
- [14] E. Gardner and B. Derrida, *Journal of Physics A: Mathematical and General* **21**, 271 (1988).
- [15] M. Talagrand, *Spin glasses: a challenge for mathematicians: cavity and mean field models*, Vol. 46 (Springer Science & Business Media, 2003).
- [16] R. Monasson and R. Zecchina, *Physical Review Letters* **75**, 2432 (1995).
- [17] D. Pollard, *A user's guide to measure theoretic probability*, Vol. 8 (Cambridge University Press, 2002).
- [18] M. Mézard, G. Parisi, and M. Virasoro, *Spin glass theory and beyond: An Introduction to the Replica Method and Its Applications*, Vol. 9 (World Scientific Publishing Company, 1987).
- [19] V. I. Bogachev, *Gaussian measures* (American Mathematical Society, 1998).
- [20] W. Kibble, *Mathematical Proceedings of the Cambridge Philosophical Society* **41**, 12 (1945).
- [21] Y. L. Tong, *The multivariate normal distribution* (Springer Science & Business Media, 2012).
- [22] M. Shcherbina and B. Tirozzi, *Communications in Mathematical Physics* **234**, 383 (2003).
- [23] J. Ding and N. Sun, in *Proceedings of the 51st Annual ACM SIGACT Symposium on Theory of Computing* (2019) pp. 816–827.
- [24] B. Aubin, A. Maillard, J. Barbier, F. Krzakala, N. Macris, and L. Zdeborová, *Journal of Statistical Mechanics: Theory and Experiment* **2019**, 124023 (2019).
- [25] R. Urbanczik, *Journal of Physics A: Mathematical and General* **30**, L387 (1997).
- [26] M. Abramowitz and I. A. Stegun, *Handbook of mathematical functions with formulas, graphs, and mathematical tables*, Vol. 55 (US Government printing office, 1948).
- [27] R. H. Byrd, J. C. Gilbert, and J. Nocedal, *Mathematical Programming* **89**, 149 (2000).
- [28] P. Poirazi, T. Brannon, and B. W. Mel, *Neuron* **37**, 989 (2003).

Appendix A: Gaussian measures, Hermite polynomials, and weak differentiability

In this appendix, we review relevant background material from the theory of Gaussian measures. Our discussion is a specialization of the more general discussion in Chapter 1 of Bogachev [19] to the one-dimensional case. We merely seek to summarize the relevant definitions and results, and will not attempt to provide rigorous proofs.

We let γ be the standard Gaussian probability measure on \mathbb{R} , which has density $\exp(-x^2/2)/\sqrt{2\pi}$ with respect to Lebesgue measure. We let $\mathcal{L}^2(\gamma)$ be the Lebesgue space of functions on \mathbb{R} that are square-integrable with respect to γ , and, for brevity, denote the norm on this space as $\|\cdot\|_\gamma$. The natural orthonormal basis for $\mathcal{L}^2(\gamma)$ is given by the set of Hermite polynomials $\{\text{He}_k\}_{k=0}^\infty$, which can be defined by the formula

$$\text{He}_k(x) = \frac{(-1)^k}{\sqrt{k!}} \exp\left(\frac{x^2}{2}\right) \frac{d^k}{dx^k} \exp\left(-\frac{x^2}{2}\right). \quad (\text{A1})$$

The Hermite polynomials satisfy the recurrence relation

$$\text{He}'_k(x) = \sqrt{k} \text{He}_{k-1}(x) = x \text{He}_k(x) - \sqrt{k+1} \text{He}_{k+1}(x) \quad (\text{A2})$$

for $k \geq 1$, with $\text{He}_0 \equiv 1$. For a given function $g \in \mathcal{L}^2(\gamma)$, we define its Fourier-Hermite coefficients

$$g_k = \int g \text{He}_k d\gamma, \quad (\text{A3})$$

and the Fourier-Hermite series

$$g(x) = \sum_{k=0}^{\infty} g_k \text{He}_k(x), \quad (\text{A4})$$

which is guaranteed to converge in mean-square by the fact that $\|g\|_\gamma^2 = \sum_{k=0}^{\infty} g_k^2$ is finite.

Then, using the recurrence relation $\text{He}'_k(x) = \sqrt{k} \text{He}_{k-1}(x)$ and the fact that $\text{He}'_0 \equiv 0$, we can express the l^{th} weak derivative of g as a formal Fourier-Hermite series

$$g^{(l)}(x) = \sum_{k=l}^{\infty} g_k \sqrt{(k)_l} \text{He}_{k-l}(x), \quad (\text{A5})$$

where $(k)_r = k(k-1)\cdots(k-r+1)$ is the falling factorial. If, for some $r \geq 0$, the sum

$$\|g^{(r)}\|_\gamma^2 = \sum_{k=r}^{\infty} (k)_r g_k^2 \quad (\text{A6})$$

is finite, then the Fourier-Hermite series for g and its weak derivatives up to order r converge in mean-square. The class of functions satisfying this condition is the Sobolev class $\mathcal{H}^r(\gamma)$, which has Sobolev norm

$$\|g\|_{\mathcal{H}^r(\gamma)} = \left(\sum_{l=0}^r \|g^{(l)}\|_\gamma^2 \right)^{1/2}. \quad (\text{A7})$$

Having defined $\mathcal{H}^r(\gamma)$ in terms of Fourier-Hermite expansions, we now connect this definition to a more generic notion of weak differentiability. Let $\mathcal{C}_0^\infty(\mathbb{R})$ be the set of all infinitely-differentiable functions with compact support, and let $p \geq 1$. For a locally integrable function f , we define its weak derivative f' as a locally integrable function that satisfies the integration by parts formula

$$\int_{\mathbb{R}} \phi'(x) f(x) dx = - \int_{\mathbb{R}} \phi(x) f'(x) dx \quad (\text{A8})$$

for every $\phi \in \mathcal{C}_0^\infty(\mathbb{R})$. The subset of functions in $\mathcal{L}^2(\mathbb{R})$ with weak derivatives up to order r of finite \mathcal{L}^2 norm forms the Sobolev class $\mathcal{H}^r(\mathbb{R})$. We can then define the class $\mathcal{H}_{\text{loc}}^r(\mathbb{R})$ as the set of all functions f on \mathbb{R} such that $\phi f \in \mathcal{H}^r(\mathbb{R})$ for all $\phi \in \mathcal{C}_0^\infty(\mathbb{R})$. $\mathcal{H}^r(\gamma)$ coincides with the class of all functions $f \in \mathcal{H}_{\text{loc}}^r(\mathbb{R})$ such that f and its weak derivatives up to order r have finite $\mathcal{L}^2(\gamma)$ norm, and the corresponding weak derivatives coincide as well. In one dimension, the criterion that the $(r-1)^{\text{th}}$ derivative is differentiable almost everywhere and is equal almost everywhere to the Lebesgue integral of its derivative implies the required weak differentiability condition. Furthermore, by Rademacher's theorem, every function that is locally Lipschitz continuous belongs to $\mathcal{H}_{\text{loc}}^1(\mathbb{R})$.

Appendix B: The Gardner volume of the treelike committee machine

In this appendix, we give a detailed account of the computation of the Gardner volume of the treelike committee machine using the replica method. As described in the main text, the treelike committee machine [9–12] is a two-layer neural network with a total of N inputs divided into disjoint groups of N/K among K hidden units:

$$y(\mathbf{x}; \{\mathbf{w}_j\}, \mathbf{v}, \vartheta) = \text{sign} \left(\frac{1}{\sqrt{K}} \sum_{j=1}^K v_j g \left(\frac{\mathbf{w}_j \cdot \mathbf{x}_j}{\sqrt{N/K}} \right) - \vartheta \right), \quad (\text{B1})$$

where $\mathbf{x}_j \in \mathbb{R}^{N/K}$ is the vector of inputs to the j^{th} hidden unit, $\{\mathbf{w}_j \in \mathbb{R}^{N/K}\}_{j=1}^K$ are the hidden unit weight vectors, $\mathbf{v} \in \mathbb{R}^K$ is the fixed readout weight vector, g is the activation function, and $\vartheta \in \mathbb{R}$ is a threshold. We want to characterize the ability of this network to classify a dataset of P independent and identically distributed random examples $\{(\mathbf{x}^\nu, y^\nu)\}_{\nu=1}^P$, where $\mathbf{x}^\nu \in \{-1, 1\}^N$ and $y^\nu \in \{-1, 1\}$, in terms of the Gardner volume [13, 14]

$$Z_{N,P,K} = \int d\rho(\{\mathbf{w}_j\}) \prod_{\nu=1}^P \Theta(y^\nu y(\mathbf{x}^\nu; \{\mathbf{w}_j\}, \mathbf{v}, \vartheta) - \kappa), \quad (\text{B2})$$

where ρ is a measure on the space of hidden unit weights. We will compute the limiting quenched free entropy per weight f in the sequential limit $N, P \rightarrow \infty$, $K \rightarrow \infty$, with load $N/P \rightarrow \alpha \in (0, \infty)$ using the replica trick as

$$f \equiv \lim_{K \rightarrow \infty} \lim_{N \rightarrow \infty} f_{N,\alpha N,K} = \lim_{K \rightarrow \infty} \lim_{N \rightarrow \infty} \frac{1}{N} \mathbb{E}_{\mathbf{x},y} \log Z_{N,\alpha N,K} = \lim_{n \downarrow 0} \lim_{K \rightarrow \infty} \lim_{N \rightarrow \infty} \frac{1}{nN} \log \mathbb{E}_{\mathbf{x},y} Z_{N,\alpha N,K}^n, \quad (\text{B3})$$

where $\mathbb{E}_{\mathbf{x},y}$ denotes expectation over the quenched Bernoulli disorder represented by the dataset.

We take the elements of \mathbf{x}^ν to be independent and identically distributed, with equal probability of being positive or negative. We allow the distribution of y^ν to be asymmetric, with $\mathbb{P}(y^\nu = +1) = 1 - \mathbb{P}(y^\nu = -1) = p$ for some $p \in [0, 1]$. We consider the case of spherical weights [9–11, 13, 14], in which the hidden unit weight vectors are uniformly distributed on the N/K -sphere of radius $(N/K)^{1/2}$. With this choice, the total volume of weight space is

$$\int d\rho = S_{N/K} (\sqrt{N/K})^K, \quad (\text{B4})$$

where

$$S_D(R) \equiv \frac{2\pi^{D/2}}{\Gamma(D/2)} R^{D-1} \quad (\text{B5})$$

is the surface area of the D -dimensional sphere of radius R . We will assume that $\|\mathbf{v}\|_2 = \sqrt{K}$, but will not initially impose further conditions on the readout weights or threshold. Finally, we assume that $g \in \mathcal{L}^2(\gamma)$.

Introducing replicas indexed by $a = 1, \dots, n$, we can write the n^{th} quenched moment of the Gardner volume as

$$\mathbb{E}_{\mathbf{x},y} Z^n = \mathbb{E}_{\mathbf{x},y} \int \prod_a d\rho(\{\mathbf{w}_j^a\}) \prod_{a,\nu} \Theta \left(y^\nu \left[\frac{1}{\sqrt{K}} \sum_j v_j g \left(\frac{\mathbf{w}_j^a \cdot \mathbf{x}_j^\nu}{\sqrt{N/K}} \right) - \vartheta \right] - \kappa \right). \quad (\text{B6})$$

We observe immediately that the fact that the different patterns are independent and identically distributed implies that

$$\mathbb{E}_{\mathbf{x},y} Z^n = \int \prod_a d\rho(\{\mathbf{w}_j^a\}) \left[\mathbb{E}_{\mathbf{x},y} \prod_a \Theta \left(y \left[\frac{1}{\sqrt{K}} \sum_j v_j g \left(\frac{\mathbf{w}_j^a \cdot \mathbf{x}_j}{\sqrt{N/K}} \right) - \vartheta \right] - \kappa \right) \right]^n, \quad (\text{B7})$$

allowing us to simplify our notation by eliminating the pattern index ν . We now consider the local fields

$$h_j^a \equiv \sqrt{\frac{K}{N}} \mathbf{w}_j^a \cdot \mathbf{x}_j, \quad (\text{B8})$$

which have mean zero and covariance

$$\text{cov}(h_j^a, h_l^b) = \delta_{jl} \frac{K}{N} \mathbf{w}_j^a \cdot \mathbf{x}_j. \quad (\text{B9})$$

In this setting, the natural order parameters are the Edwards-Anderson (EA) order parameters [13, 15, 18]

$$q_j^{ab} \equiv \frac{K}{N} \mathbf{w}_j^a \cdot \mathbf{w}_j^b \quad (a \neq b), \quad (\text{B10})$$

which measure the overlap between the weight vectors of each hidden unit in two different replicas. As we have chosen the weight vectors to lie on the sphere, the self-overlap of each hidden unit is fixed to unity, and the EA order parameters are bounded between negative one and one. In terms of the EA order parameters, we have

$$\text{cov}(h_j^a, h_l^b) = \delta_{jl}[\delta_{ab} + q_j^{ab}(1 - \delta_{ab})]. \quad (\text{B11})$$

Then, as each of the local fields is the sum of N/K independent random variables and their covariance is finite, by central limit theorem they converge in distribution as $N \rightarrow \infty$ for any fixed K to a multivariate Gaussian with the same mean and covariance [17, 21]. We note that this limiting result would alternatively follow by inserting Fourier representations of the delta function to enforce the definition of the variables h_j^a , evaluating the averages over the inputs, and expanding the result to lowest order in $1/N$.

We then define the function

$$G_1(\{q_j^{ab}\}) \equiv \frac{1}{n} \log \mathbb{E}_y \mathbb{E}_h \prod_a \Theta \left(y \left[\frac{1}{\sqrt{K}} \sum_j v_j g(h_j^a) - \vartheta \right] - \kappa \right), \quad (\text{B12})$$

where the average \mathbb{E}_h is taken over the q_j^{ab} -dependent Gaussian distribution of the local fields. Introducing Lagrange multipliers \hat{q}_j^{ab} to enforce the definitions of the order parameters q_j^{ab} , we obtain

$$\mathbb{E}_{\mathbf{x}, y} Z^n = \int \prod_{b < a, j} \frac{dq_j^{ab} d\hat{q}_j^{ab}}{2\pi i K/N} \exp \left(-\frac{N}{K} \sum_{b < a, j} q_j^{ab} \hat{q}_j^{ab} + N n \alpha G_1(\{q_j^{ab}\}) \right) \int \prod_a d\rho(\{\mathbf{w}_j^a\}) \exp \left(\sum_{b < a, j} \hat{q}_j^{ab} \mathbf{w}_j^a \cdot \mathbf{w}_j^b \right), \quad (\text{B13})$$

where we have, by convention, rescaled the Lagrange multipliers to absorb the factor of K/N in the definition of the order parameters [13]. With the choice that the weight vectors of each branch are uniformly distributed on the N/K -sphere of radius $\sqrt{N/K}$, the integral over the weights expands as

$$\int \prod_{a, j} d\mathbf{w}_j^a \left[\prod_{a, j} \delta \left(\|\mathbf{w}_j^a\|^2 - \frac{N}{K} \right) \right] \exp \left(\sum_{b < a, j} \hat{q}_j^{ab} \mathbf{w}_j^a \cdot \mathbf{w}_j^b \right). \quad (\text{B14})$$

To enforce this normalization constraint, we introduce Lagrange multipliers \hat{E}_j^a , allowing us to factor the integrals over the input dimensions of each branch. Then, defining the function G_2 by

$$nK G_2(\{q_j^{ab}\}, \{\hat{q}_j^{ab}\}, \{\hat{E}_j^a\}) \equiv \frac{1}{2} \sum_{a, j} \hat{E}_j^a - \sum_{b < a, j} q_j^{ab} \hat{q}_j^{ab} + \sum_j \log \int \prod_a d\mathbf{w}_j^a \exp \left(-\frac{1}{2} \sum_a \hat{E}_j^a (w_j^a)^2 + \sum_{b < a} \hat{q}_j^{ab} w_j^a w_j^b \right), \quad (\text{B15})$$

we can write

$$\mathbb{E}_{\mathbf{x}, y} Z^n = \int \prod_{a, j} \frac{d\hat{E}_j^a}{4\pi i} \int \prod_{b < a, j} \frac{dq_j^{ab} d\hat{q}_j^{ab}}{2\pi i K/N} \exp \left(N n \left[\alpha G_1(\{q_j^{ab}\}) + G_2(\{q_j^{ab}\}, \{\hat{q}_j^{ab}\}, \{\hat{E}_j^a\}) \right] \right). \quad (\text{B16})$$

In the limit $N \rightarrow \infty$, we can evaluate the integrals over the order parameters and the Lagrange multipliers using the method of steepest descent, which yields an expression for the quenched free entropy as

$$f = \lim_{n \downarrow 0} \text{extr}_{\{q_j^{ab}\}, \{\hat{q}_j^{ab}\}, \{\hat{E}_j^a\}} \left\{ \alpha G_1(\{q_j^{ab}\}) + G_2(\{q_j^{ab}\}, \{\hat{q}_j^{ab}\}, \{\hat{E}_j^a\}) \right\}. \quad (\text{B17})$$

We note that the function G_1 represents the energetic contribution to the quenched free entropy, while the function G_2 represents the entropic contribution.

Appendix C: Replica-symmetric solution

In this appendix, we study the quenched free entropy derived in Appendix B using a replica-symmetric ansatz [12–15, 18]. In addition, as we expect the different hidden units to be equivalent to one another after averaging over patterns [10, 11], we make the ansatz that the order parameters are the same across all hidden units. Concretely, we make the ansatz

$$\begin{cases} \hat{E}_j^a = \hat{E} \\ q_j^{ab} = q \\ \hat{q}_j^{ab} = \hat{q} \end{cases} \quad (\text{C1})$$

which substantially simplifies the saddle point equations.

1. The replica-symmetric quenched free entropy

Considering the entropic contribution G_2 , we immediately obtain the simplification

$$G_2 = \frac{1}{2}\hat{E} - \frac{1}{2}(n-1)q\hat{q} + \frac{1}{n} \log \int d^n w \exp\left(-\frac{1}{2}\mathbf{w}^T \mathbf{A} \mathbf{w}\right), \quad (\text{C2})$$

where we have defined the $n \times n$ matrix

$$\mathbf{A} = (\hat{E} + \hat{q})\mathbf{I}_n - \hat{q}\mathbf{1}_n\mathbf{1}_n^T. \quad (\text{C3})$$

Applying the matrix determinant lemma, we have

$$\det \mathbf{A} = (\hat{E} + \hat{q})^n \left(1 - \frac{\hat{q}}{\hat{E} + \hat{q}}n\right), \quad (\text{C4})$$

hence we find that

$$\lim_{n \downarrow 0} \frac{1}{n} \log \int d^n w \exp\left(-\frac{1}{2}\mathbf{w}^T \mathbf{A} \mathbf{w}\right) = \frac{1}{2} \left[\log \frac{2\pi}{\hat{E} + \hat{q}} + \frac{\hat{q}}{\hat{E} + \hat{q}} \right]. \quad (\text{C5})$$

Then, as we would expect, the entropic contribution to the quenched free entropy is the same as for a perceptron [13], yielding

$$\lim_{n \downarrow 0} G_2 = \frac{1}{2} \left[\hat{E} + q\hat{q} + \log \frac{2\pi}{\hat{E} + \hat{q}} + \frac{\hat{q}}{\hat{E} + \hat{q}} \right]. \quad (\text{C6})$$

As the Lagrange multipliers \hat{E} and \hat{q} appear only in G_2 , they can easily be eliminated from the saddle point equations, yielding

$$\lim_{n \downarrow 0} G_2 = \frac{1}{2} \left[\frac{1}{1-q} + \log[2\pi(1-q)] \right] \quad (\text{C7})$$

at the replica-symmetric saddle point.

We now consider the energetic term G_1 . With the replica- and branch-symmetric ansatz, the covariance matrix of the Gaussian-distributed local fields simplifies to

$$\text{cov}(h_j^a, h_l^b) = \delta_{jl}[\delta_{ab} + q(1 - \delta_{ab})]. \quad (\text{C8})$$

Then, as the local fields h_j are independent, the internal fields

$$s^a \equiv \frac{1}{\sqrt{K}} \sum_j v_j g(h_j^a) - \vartheta \quad (\text{C9})$$

are the sums of K independent random variables, with mean

$$\mu \equiv \mathbb{E}_h s^a = \left[\frac{1}{\sqrt{K}} \sum_j v_j \right] (\mathbb{E}g) - \vartheta \quad (\text{C10})$$

and covariance

$$\text{cov}(s^a, s^b) = \frac{1}{K} \sum_{j,l=1}^K v_j v_l \text{cov}(g(h_j^a), g(h_l^b)) = \frac{1}{K} \sum_{j=1}^K v_j^2 \text{cov}(g(h_j^a), g(h_j^b)) = \text{cov}(g(h^a), g(h^b)) \quad (\text{C11})$$

where we have used the fact the fields are independent and identically distributed across branches and the assumption that $\|\mathbf{v}\|_2^2 = K$. Then, if $\text{cov}(g(h^a), g(h^b))$ is finite, which holds for any $g \in \mathcal{L}^2(\gamma)$, then the classical central limit theorem implies that the internal fields s^a converge in distribution as $K \rightarrow \infty$ to a multivariate Gaussian with the mean and variance given above [17, 21].

Defining the quantity

$$\sigma^2 \equiv \text{var}[g(x) : x \sim \mathcal{N}(0, 1)] = \|g\|_\gamma^2 - (\mathbb{E}g)^2 \quad (\text{C12})$$

and the effective order parameter

$$\tilde{q} = \text{cov} \left[g(x), g(y) ; \begin{bmatrix} x \\ y \end{bmatrix} \sim \mathcal{N} \left(0, \begin{bmatrix} 1 & q \\ q & 1 \end{bmatrix} \right) \right], \quad (\text{C13})$$

we can see from the joint distribution of the local fields h^a that we can write the covariance matrix of the internal fields as

$$\text{cov}(s^a, s^b) = \sigma^2 \delta_{ab} + \tilde{q}(1 - \delta_{ab}). \quad (\text{C14})$$

Then, we can expand the first average in $\exp(nG_1)$ in terms of the joint characteristic function of s^a as

$$\int \prod_a \frac{ds^a d\hat{s}^a}{2\pi} \left[\prod_a \Theta(-s^a - \kappa) \right] \exp \left(i \sum_a s^a \hat{s}^a - \frac{1}{2}(\sigma^2 - \tilde{q}) \sum_a (\hat{s}^a)^2 - \frac{1}{2} \tilde{q} \left[\sum_a \hat{s}^a \right]^2 + i\mu \sum_a \hat{s}^a \right). \quad (\text{C15})$$

To evaluate the remaining integrals, we perform a Hubbard-Stratonovich transformation, which is defined via the integral identity [12]

$$\exp \left(-\frac{1}{2} x^2 \right) = \int d\gamma(z) \exp(-ixz), \quad (\text{C16})$$

to decouple the replicas at the expense of introducing an auxiliary field z . From a statistical point of view, we can see that this has the effect of shifting the mean of s^a from μ to $\mu + \sqrt{\tilde{q}}z$, which yields

$$\int d\gamma(z) \left[\int \frac{ds d\hat{s}}{2\pi} \Theta(-s - \kappa) \exp \left(is\hat{s} - \frac{1}{2}(\sigma^2 - \tilde{q})\hat{s}^2 + i(\mu + \sqrt{\tilde{q}}z)\hat{s} \right) \right]^n \quad (\text{C17})$$

$$= \int d\gamma(z) \left[H \left(\frac{\kappa + \mu + \sqrt{\tilde{q}}z}{\sqrt{\sigma^2 - \tilde{q}}} \right) \right]^n, \quad (\text{C18})$$

where $H(z) = \int_z^\infty d\gamma(x)$ is the Gaussian tail distribution function. Analogously, we can see that the second term in $\exp(nG_1)$ can be written in a similar form, yielding

$$\exp(nG_1) = (1-p) \int d\gamma(z) \left[H \left(\frac{\kappa + \mu + \sqrt{\tilde{q}}z}{\sqrt{\sigma^2 - \tilde{q}}} \right) \right]^n + p \int d\gamma(z) \left[H \left(\frac{\kappa - \mu - \sqrt{\tilde{q}}z}{\sqrt{\sigma^2 - \tilde{q}}} \right) \right]^n. \quad (\text{C19})$$

Applying the identity

$$\mathbb{E} \log x = \lim_{n \downarrow 0} \frac{\log(\mathbb{E}x^n)}{n}, \quad (\text{C20})$$

upon passing to the limit $n \downarrow 0$ we obtain the replica-symmetric free entropy

$$f_{\text{RS}} = \text{extr}_q \left\{ (1-p)\alpha \int d\gamma(z) \log H \left(\frac{\kappa + \mu + \sqrt{\tilde{q}}z}{\sqrt{\sigma^2 - \tilde{q}}} \right) + p\alpha \int d\gamma(z) \log H \left(\frac{\kappa - \mu - \sqrt{\tilde{q}}z}{\sqrt{\sigma^2 - \tilde{q}}} \right) + \frac{1}{2} \left[\frac{1}{1-q} + \log(1-q) + \log(2\pi) \right] \right\}. \quad (\text{C21})$$

2. The replica-symmetric capacity

The replica-symmetric capacity α_{RS} is determined by the value of α such that $q \uparrow 1$ [9–14]. Solving the saddle point equation for q from the replica-symmetric free entropy f_{RS} for α^{-1} , we have

$$\frac{1}{\alpha_{\text{RS}}} = \lim_{q \uparrow 1} \frac{(1-q)^2}{q} \frac{\partial \tilde{q}}{\partial q} \left[(1-p) \int d\gamma(z) \frac{1}{H(c_+)} \frac{1}{\sqrt{2\pi}} \exp\left(-\frac{c_+^2}{2}\right) \frac{1}{(\sigma^2 - \tilde{q})^{3/2}} \left(\kappa + \mu + \frac{z\sigma^2}{\sqrt{\tilde{q}}}\right) \right. \\ \left. + p \int d\gamma(z) \frac{1}{H(c_-)} \frac{1}{\sqrt{2\pi}} \exp\left(-\frac{c_-^2}{2}\right) \frac{1}{(\sigma^2 - \tilde{q})^{3/2}} \left(\kappa - \mu - \frac{z\sigma^2}{\sqrt{\tilde{q}}}\right) \right], \quad (\text{C22})$$

where, for brevity, we write

$$c_{\pm} \equiv \frac{\kappa \pm \mu \pm \sqrt{\tilde{q}}z}{\sqrt{\sigma^2 - \tilde{q}}}. \quad (\text{C23})$$

We can then see that the finiteness of the replica-symmetric critical capacity depends on the analytic properties of \tilde{q} in the limit $q \uparrow 1$. To study the properties of this limit, we make the change of variables $q = 1 - \varepsilon$. We generically expect $\tilde{q} \uparrow \sigma^2$, but the way in which \tilde{q} approaches σ^2 depends on the activation function. As observed by Baldassi *et al.* [9], for $g(x) = \text{sign}(x)$, $\sigma^2 - \tilde{q} \sim \sqrt{\varepsilon}$, while, for $g(x) = \text{ReLU}(x)$, $\sigma^2 - \tilde{q} \sim \varepsilon$. As shown in the main text, the asymptotic scaling $\sigma^2 - \tilde{q} \sim \varepsilon$ holds for all $g \in \mathcal{H}^1(\gamma)$. We thus make the ansatz

$$\tilde{q} \sim \sigma^2 - \beta\varepsilon^\ell \quad (\text{C24})$$

for some parameters $\beta, \ell > 0$. Then, the contribution of the first term in the saddle point equation above to α_{RS}^{-1} is given to leading order as

$$\frac{\varepsilon^{1-\ell/2}}{1-\varepsilon} \frac{\ell(1-p)}{\sqrt{\beta}} \int d\gamma(z) \frac{1}{H(c_+)} \frac{1}{\sqrt{2\pi}} \exp\left(-\frac{c_+^2}{2}\right) \frac{1}{(\sigma^2 - \tilde{q})^{3/2}} \left(\kappa + \mu + \frac{z\sigma^2}{\sqrt{\sigma^2 - \beta\varepsilon^\ell}}\right), \quad (\text{C25})$$

where we have reparameterized c_+ in terms of ε . In the limit $\varepsilon \downarrow 0$, c_+ tends to $+\infty$ if $z \geq -(\kappa + \mu)/\sigma$ and to $-\infty$ otherwise. Noting that

$$\frac{1}{H(x)} \sim \begin{cases} 1 + (2\pi x^2)^{-1/2} \exp(-x^2/2) [1 - x^{-2} + \mathcal{O}(x^{-4})] & x \ll -1 \\ \sqrt{2\pi} x \exp(x^2/2) [1 + x^{-2} + \mathcal{O}(x^{-4})] & x \gg +1 \end{cases}, \quad (\text{C26})$$

we can see that the only non-vanishing contribution comes from the interval $z \geq -(\kappa + \mu)/\sigma$. Thus, to leading order, this term is given as

$$\frac{\varepsilon^{1-\ell}}{1-\varepsilon} \frac{\ell(1-p)}{\beta} \int_{-(\kappa+\mu)/\sigma}^{\infty} d\gamma(z) \left(\kappa + \mu + z\sqrt{\sigma^2 - \beta\varepsilon^\ell}\right) \left(\kappa + \mu + \frac{z\sigma^2}{\sqrt{\sigma^2 - \beta\varepsilon^\ell}}\right), \quad (\text{C27})$$

which we can further approximate as

$$\ell\varepsilon^{1-\ell} \frac{1-p}{\beta} \int_{-(\kappa+\mu)/\sigma}^{\infty} d\gamma(z) (\kappa + \mu + \sigma z). \quad (\text{C28})$$

By an identical procedure, we can derive the leading-order contribution to the second term, in which case the non-vanishing contribution to the integral comes from $z \leq (\kappa - \mu)/\sigma$, yielding

$$\frac{1}{\alpha_{\text{RS}}} = \lim_{\varepsilon \downarrow 0} \ell\varepsilon^{1-\ell} \left[\frac{1-p}{\beta} \int_{-(\kappa+\mu)/\sigma}^{\infty} d\gamma(z) (\kappa + \mu + \sigma z) + \frac{p}{\beta} \int_{-\infty}^{(\kappa-\mu)/\sigma} d\gamma(z) (\kappa - \mu - \sigma z) \right]. \quad (\text{C29})$$

We note that this result can alternatively be obtained using the method of Engel *et al.* [11], which exploits the properties of the function whose extremum with respect to q defines the free entropy f_{RS} to avoid the need to explicitly compute the saddle point equation.

Thus, we can see that the limit $\varepsilon \downarrow 0$ vanishes for $\ell < 1$, implying divergence of the replica-symmetric capacity. If $\ell \geq 1$, which holds for all functions $g \in \mathcal{H}^1(\gamma)$, the capacity remains finite, and we have $\beta = \|g'\|_\gamma^2$. We note that the

boundary case $\ell = 1$, which corresponds to non-zero $\|g'\|_\gamma^2$, is special, as the capacity vanishes if $\ell > 1$. For this class of functions, we therefore obtain

$$\frac{1}{\alpha_{\text{RS}}} = \frac{\sigma^2}{\|g'\|_\gamma^2} \left[(1-p) \int_{-(\kappa+\mu)/\sigma}^{\infty} d\gamma(z) \left(\frac{\kappa+\mu}{\sigma} + z \right)^2 + p \int_{-(\kappa-\mu)/\sigma}^{\infty} d\gamma(z) \left(\frac{\kappa-\mu}{\sigma} + z \right)^2 \right]. \quad (\text{C30})$$

By inspection, we can see that if $p = 1/2$ and the output distribution is symmetric, α_{RS} is maximized by taking $\mu = 0$. If the condition $\mu = 0$ holds, the formula above simplifies to

$$\frac{1}{\alpha_{\text{RS}}} = \frac{\sigma^2}{\|g'\|_\gamma^2} \int_{-\kappa/\sigma}^{\infty} d\gamma(z) (\kappa/\sigma + z)^2, \quad (\text{C31})$$

as given in the main text.

Appendix D: One-step replica-symmetry-breaking solution

In this appendix, we consider a one-step replica-symmetry-breaking (1-RSB) ansatz, in which we divide the n replicas into groups of size m , known as the Parisi parameter, and allow the overlaps between groups to differ from the overlaps within groups [9–12, 15, 18]. Again, we assume that the order parameters are translation-invariant across branches. We let q_0 denote the overlaps between replicas in different groups, and q_1 the overlap between replicas within the same group, with corresponding Lagrange multipliers \hat{q}_0 and \hat{q}_1 .

1. The 1-RSB quenched free entropy

With the 1-RSB ansatz, the entropic contribution G_2 simplifies to

$$G_2 = \frac{1}{2} \hat{E} - \frac{1}{2} (n-m) q_0 \hat{q}_0 - \frac{1}{2} (m-1) q_1 \hat{q}_1 + \frac{1}{n} \log \int d^n w \exp \left(-\frac{1}{2} \mathbf{w}^T \mathbf{C} \mathbf{w} \right), \quad (\text{D1})$$

where we have defined the $n \times n$ block Toeplitz matrix

$$\mathbf{C} = \begin{pmatrix} \mathbf{A} & \mathbf{B} & \cdots & \mathbf{B} \\ \mathbf{B} & \mathbf{A} & \ddots & \vdots \\ \vdots & \ddots & \ddots & \vdots \\ \mathbf{B} & \cdots & & \mathbf{A} \end{pmatrix}, \quad (\text{D2})$$

where the $m \times m$ blocks are defined as

$$\mathbf{A} = (\hat{E} + \hat{q}_1) \mathbf{I}_m - \hat{q}_1 \mathbf{1}_m \mathbf{1}_m^T \quad (\text{D3})$$

and

$$\mathbf{B} = -\hat{q}_0 \mathbf{1}_m \mathbf{1}_m^T, \quad (\text{D4})$$

respectively. Then, as the integral over \mathbf{w} is Gaussian, it can easily be evaluated, yielding

$$\frac{1}{n} \log \int d^n w \exp \left(-\frac{1}{2} \mathbf{w}^T \mathbf{C} \mathbf{w} \right) = \frac{1}{2} \log(2\pi) - \frac{1}{2n} \log \det \mathbf{C}. \quad (\text{D5})$$

To compute the determinant of \mathbf{C} , we will use a convenient lemma. For n/m a power of two, we have

$$\det \mathbf{C} = \det(\mathbf{A} - \mathbf{B})^{n/m-1} \det(\mathbf{A} + (n/m - 1)\mathbf{B}), \quad (\text{D6})$$

which follows from the identity

$$\det \begin{pmatrix} \mathbf{A} & \mathbf{B} \\ \mathbf{B} & \mathbf{A} \end{pmatrix} = \det(\mathbf{A} - \mathbf{B}) \det(\mathbf{A} + \mathbf{B}), \quad (\text{D7})$$

and induction on n/m in powers of two. By the matrix determinant lemma, we have

$$\det(\mathbf{A} - \mathbf{B}) = (\hat{E} + \hat{q}_1)^m \left(1 + m \frac{\hat{q}_0 - \hat{q}_1}{\hat{E} + \hat{q}_1} \right) \quad (\text{D8})$$

and

$$\det(\mathbf{A} + (n/m - 1)\mathbf{B}) = (\hat{E} + \hat{q}_1)^m \left(1 + m \frac{(1 - n/m)\hat{q}_0 - \hat{q}_1}{\hat{E} + \hat{q}_1} \right). \quad (\text{D9})$$

Therefore, for n/m a power of two, we have

$$\frac{1}{n} \log \det \mathbf{C} = \log(\hat{E} + \hat{q}_1) + \frac{n - m}{nm} \log \left(1 + m \frac{\hat{q}_0 - \hat{q}_1}{\hat{E} + \hat{q}_1} \right) + \frac{1}{n} \log \left(1 + \frac{(m - n)\hat{q}_0 - m\hat{q}_1}{\hat{E} + \hat{q}_1} \right). \quad (\text{D10})$$

Assuming the validity of analytic continuation to $n \downarrow 0$, we have

$$\lim_{n \downarrow 0} \log \det \mathbf{C} = \log(\hat{E} + \hat{q}_1) - \frac{\hat{q}_0}{\hat{E} + \hat{q}_1 + m(\hat{q}_0 - \hat{q}_1)} + \frac{1}{m} \log \left(\frac{\hat{E} + \hat{q}_1 + m(\hat{q}_0 - \hat{q}_1)}{\hat{E} + \hat{q}_1} \right). \quad (\text{D11})$$

Therefore, we obtain

$$\begin{aligned} \lim_{n \downarrow 0} G_2 &= \frac{1}{2} \hat{E} + \frac{1}{2} q_1 \hat{q}_1 + \frac{1}{2} m (q_0 \hat{q}_0 - q_1 \hat{q}_1) \\ &+ \frac{1}{2} \left[\log \left(\frac{2\pi}{\hat{E} + \hat{q}_1} \right) + \frac{\hat{q}_0}{\hat{E} + \hat{q}_1 + m(\hat{q}_0 - \hat{q}_1)} + \frac{1}{m} \log \left(\frac{\hat{E} + \hat{q}_1}{\hat{E} + \hat{q}_1 + m(\hat{q}_0 - \hat{q}_1)} \right) \right]. \end{aligned} \quad (\text{D12})$$

We note that this result can alternatively be obtained with substantially more algebra by performing many Hubbard-Stratonovich transformations [11]. As the Lagrange multipliers \hat{E} , \hat{q}_0 , and \hat{q}_1 appear only in G_2 , we can eliminate them from the saddle point equations, yielding

$$\lim_{n \downarrow 0} G_2 = \frac{1}{2} \left[1 + \frac{q_0}{1 - q_1 - m(q_0 - q_1)} + \log[2\pi(1 - q_1)] + \frac{1}{m} \log \left(\frac{1 - q_1 - m(q_0 - q_1)}{1 - q_1} \right) \right] \quad (\text{D13})$$

at the 1-RSB saddle point, which reduces to the replica-symmetric result if we take $q_0 = q_1$.

We now consider the energetic contribution G_1 . As in the replica-symmetric case, the central limit theorem implies that the internal fields

$$s^a \equiv \frac{1}{\sqrt{K}} \sum_j v_j g(h_j^a) - \vartheta \quad (\text{D14})$$

converge in distribution to a Gaussian as $K \rightarrow \infty$. Their mean μ is the same as before, but now their covariance is given by the block Toeplitz matrix

$$\mathbf{C} = \begin{pmatrix} \mathbf{A} & \mathbf{B} & \cdots & \mathbf{B} \\ \mathbf{B} & \mathbf{A} & \ddots & \vdots \\ \vdots & \ddots & \ddots & \vdots \\ \mathbf{B} & \cdots & & \mathbf{A} \end{pmatrix}, \quad (\text{D15})$$

with $m \times m$ blocks

$$\mathbf{A} = (\sigma^2 - \tilde{q}_1) \mathbf{I}_m + \tilde{q}_1 \mathbf{1}_m \mathbf{1}_m^T \quad (\text{D16})$$

and

$$\mathbf{B} = \tilde{q}_0 \mathbf{1}_m \mathbf{1}_m^T, \quad (\text{D17})$$

where $\sigma^2 = \text{var}[g(h)]$ as before and the effective order parameter now takes two values

$$\tilde{q}_j = \text{cov} \left[g(x), g(y); \begin{bmatrix} x \\ y \end{bmatrix} \sim \mathcal{N} \left(0, \begin{bmatrix} 1 & q_j \\ q_j & 1 \end{bmatrix} \right) \right], \quad j = 1, 2. \quad (\text{D18})$$

We now want to understand the structure of the joint characteristic function of the replicated internal fields, in terms of which we will expand G_1 , such that we can decouple replicas by performing appropriate Hubbard-Stratonovich transformations. Introducing Lagrange multipliers $\hat{\mathbf{s}}$ and indexing blocks by Greek superscripts, we have

$$\hat{\mathbf{s}} \cdot \mathbf{C}\hat{\mathbf{s}} = \sum_{\lambda=1}^{n/m} \hat{\mathbf{s}}^\lambda \cdot \mathbf{A}\hat{\mathbf{s}}^\lambda + \sum_{\nu \neq \lambda} \hat{\mathbf{s}}^\nu \cdot \mathbf{B}\hat{\mathbf{s}}^\lambda = (\sigma^2 - \tilde{q}_1)(\hat{\mathbf{s}} \cdot \hat{\mathbf{s}}) + (\tilde{q}_1 - \tilde{q}_0) \sum_{\lambda=1}^{n/m} (\mathbf{1}_m \cdot \hat{\mathbf{s}}^\lambda)^2 + \tilde{q}_0 (\mathbf{1}_n \cdot \hat{\mathbf{s}})^2. \quad (\text{D19})$$

Then, we can see that we will need to perform one Hubbard-Stratonovich transformation to decouple the $(\mathbf{1}_n \cdot \hat{\mathbf{s}})^2$ term at the expense of introducing an auxiliary field z_0 , which has the effect of shifting the mean of s^a from μ to $\mu + \sqrt{\tilde{q}_0}z_0$. To decouple the $(\mathbf{1}_m \cdot \hat{\mathbf{s}}^\lambda)^2$ terms, we introduce n/m auxiliary fields z_1^λ , which further shifts the mean of s^a from $\mu + \sqrt{\tilde{q}_0}z_0$ to $\mu + \sqrt{\tilde{q}_0}z_0 + \sqrt{\tilde{q}_1 - \tilde{q}_0}z_1^\lambda$. Then, recognizing that the contribution of each replica within a block to the integral over the corresponding z_1^λ is identical, and that the contribution of each block to the integral over z_0 is in turn identical, the first average in $\exp(nG_1)$ is given as

$$\int d\gamma(z_0) \left\{ \int d\gamma(z_1) \left[\int \frac{ds d\hat{\mathbf{s}}}{2\pi} \Theta(-s - \kappa) \exp \left(is\hat{\mathbf{s}} - \frac{1}{2}(\sigma^2 - \tilde{q}_1)\hat{\mathbf{s}}^2 + i(\mu + \sqrt{\tilde{q}_0}z_0 + \sqrt{\tilde{q}_1 - \tilde{q}_0}z_1)\hat{\mathbf{s}} \right) \right]^m \right\}^{n/m} \quad (\text{D20})$$

$$= \int d\gamma(z_0) \left\{ \int d\gamma(z_1) \left[H \left(\frac{\kappa + (\mu + \sqrt{\tilde{q}_0}z_0 + \sqrt{\tilde{q}_1 - \tilde{q}_0}z_1)}{\sqrt{\sigma^2 - \tilde{q}_1}} \right) \right]^m \right\}^{n/m}. \quad (\text{D21})$$

Analogously, we can see that the second term in $\exp(nG_1)$ can be written in a similar form, yielding

$$\begin{aligned} \exp(nG_1) &= (1-p) \int d\gamma(z_0) \left\{ \int d\gamma(z_1) \left[H \left(\frac{\kappa + (\mu + \sqrt{\tilde{q}_0}z_0 + \sqrt{\tilde{q}_1 - \tilde{q}_0}z_1)}{\sqrt{\sigma^2 - \tilde{q}_1}} \right) \right]^m \right\}^{n/m} \\ &\quad + p \int d\gamma(z_0) \left\{ \int d\gamma(z_1) \left[H \left(\frac{\kappa - (\mu + \sqrt{\tilde{q}_0}z_0 + \sqrt{\tilde{q}_1 - \tilde{q}_0}z_1)}{\sqrt{\sigma^2 - \tilde{q}_1}} \right) \right]^m \right\}^{n/m}. \end{aligned} \quad (\text{D22})$$

Therefore, passing to the limit $n \downarrow 0$, we obtain the 1-RSB saddle point free entropy

$$\begin{aligned} f_{1\text{-RSB}} &= \text{extr}_{q_0, q_1, m} \left\{ \frac{1}{m} (1-p)\alpha \int d\gamma(z_0) \log \int d\gamma(z_1) \left[H \left(\frac{\kappa + (\mu + \sqrt{\tilde{q}_0}z_0 + \sqrt{\tilde{q}_1 - \tilde{q}_0}z_1)}{\sqrt{\sigma^2 - \tilde{q}_1}} \right) \right]^m \right. \\ &\quad + \frac{1}{m} p\alpha \int d\gamma(z_0) \log \int d\gamma(z_1) \left[H \left(\frac{\kappa - (\mu + \sqrt{\tilde{q}_0}z_0 + \sqrt{\tilde{q}_1 - \tilde{q}_0}z_1)}{\sqrt{\sigma^2 - \tilde{q}_1}} \right) \right]^m \\ &\quad \left. + \frac{1}{2} \left[1 + \frac{q_0}{1 - q_1 - m(q_0 - q_1)} + \log[2\pi(1 - q_1)] + \frac{1}{m} \log \left(\frac{1 - q_1 - m(q_0 - q_1)}{1 - q_1} \right) \right] \right\}. \end{aligned} \quad (\text{D23})$$

2. The 1-RSB capacity

To determine the capacity under the 1-RSB ansatz, we need to find the value of α such that $q_1 \uparrow 1$. In this limit, we expect $m \downarrow 0$ such that the non-negative quantity

$$r \equiv \frac{m}{1 - q_1} \quad (\text{D24})$$

remains finite [9–12, 15]. We thus re-parameterize the saddle point equations by writing $q_1 = 1 - \varepsilon$ and $m = r\varepsilon$, which yields

$$\begin{aligned} f_{1\text{-RSB}} &= \text{extr}_{q_0, \varepsilon, r} \frac{1}{\varepsilon} \left\{ \frac{1}{r} (1-p)\alpha \int d\gamma(z_0) \log \int d\gamma(z_1) \left[H \left(\frac{\kappa + (\mu + \sqrt{\tilde{q}_0}z_0 + \sqrt{\tilde{q}_1 - \tilde{q}_0}z_1)}{\sqrt{\sigma^2 - \tilde{q}_1}} \right) \right]^{r\varepsilon} \right. \\ &\quad + \frac{1}{r} p\alpha \int d\gamma(z_0) \log \int d\gamma(z_1) \left[H \left(\frac{\kappa - (\mu + \sqrt{\tilde{q}_0}z_0 + \sqrt{\tilde{q}_1 - \tilde{q}_0}z_1)}{\sqrt{\sigma^2 - \tilde{q}_1}} \right) \right]^{r\varepsilon} \\ &\quad \left. + \frac{1}{2} \left[\varepsilon + \frac{q_0}{1 + r(1 - q_0 - \varepsilon)} + \varepsilon \log(2\pi\varepsilon) + \frac{1}{r} \log(1 + r(1 - q_0 - \varepsilon)) \right] \right\}, \end{aligned} \quad (\text{D25})$$

where \tilde{q}_1 is now a function of ε alone.

To derive a formula for the 1-RSB critical capacity, we follow the method used by Engel *et al.* [11]. This method starts by observing that the quantity inside the curly braces above must vanish in the limit $\varepsilon \downarrow 0$ in order for the extremum with respect to ε to be well-defined in this limit. This condition gives an implicit expression for $\alpha_{1\text{-RSB}}$ as

$$0 = \min_{q_0, r} \left\{ \frac{q_0}{1+r(1-q_0)} + \frac{1}{r} \log(1+r(1-q_0)) - \frac{2}{r} \alpha_{1\text{-RSB}} \psi(q_0, r) \right\}, \quad (\text{D26})$$

where

$$\psi(q_0, r; \kappa) \equiv -\lim_{\varepsilon \downarrow 0} \left\{ (1-p) \int d\gamma(z_0) \log \int d\gamma(z_1) [H(c_+)]^{r\varepsilon} + p \int d\gamma(z_0) \log \int d\gamma(z_1) [H(c_-)]^{r\varepsilon} \right\}, \quad (\text{D27})$$

and, for brevity, we write

$$c_{\pm} = \frac{\kappa \pm (\mu + \sqrt{\tilde{q}_0} z_0 + \sqrt{\tilde{q}_1 - \tilde{q}_0} z_1)}{\sqrt{\sigma^2 - \tilde{q}_1}}. \quad (\text{D28})$$

As $\psi \geq 0$ for all q_0, r , and κ , we can explicitly express the capacity as

$$\alpha_{1\text{-RSB}}(\kappa) = \min_{q_0, r} \left\{ \frac{1}{2\psi(q_0, r; \kappa)} \left[\frac{r q_0}{1+r(1-q_0)} + \log(1+r(1-q_0)) \right] \right\}. \quad (\text{D29})$$

We note that one could obtain the same formula for α as a function of the saddle-point values of q_0 and r by solving the saddle-point equation for ε for α and taking the limit $\varepsilon \downarrow 0$.

We must now evaluate the limit $\varepsilon \downarrow 0$ in the definition of ψ . Following our analysis of the RS critical capacity, we focus on the symmetric case $\mu = 0$, and make the ansatz that $\tilde{q}_0 \sim \sigma^2 - \beta\varepsilon^\ell$ for some $\beta, \ell > 0$. The assumption of symmetry yields the simplification

$$\psi(q_0, r; \kappa) = -\lim_{\varepsilon \downarrow 0} \int d\gamma(z_0) \log \int d\gamma(z_1) \left[H \left(\frac{\kappa + \sqrt{\tilde{q}_0} z_0 + \sqrt{\tilde{q}_1 - \tilde{q}_0} z_1}{\sqrt{\sigma^2 - \tilde{q}_1}} \right) \right]^{r\varepsilon}. \quad (\text{D30})$$

Expanding the argument of H to leading order in ε , we have

$$\frac{\kappa + \sqrt{\tilde{q}_0} z_0 + \sqrt{\tilde{q}_1 - \tilde{q}_0} z_1}{\sqrt{\sigma^2 - \tilde{q}_1}} \sim \frac{\kappa + \sqrt{\tilde{q}_0} z_0 + \sqrt{\sigma^2 - \tilde{q}_0} z_1}{\sqrt{\beta\varepsilon^\ell}}, \quad (\text{D31})$$

hence the argument of H tends to $+\infty$ for $z_1 \geq -(\kappa + \sqrt{\tilde{q}_0} z_0)/\sqrt{\sigma^2 - \tilde{q}_0}$ and to $-\infty$ otherwise. Noting that

$$H(x) \sim \begin{cases} 1 - (2\pi x^2)^{-1/2} \exp(-x^2/2) [1 - x^{-2} + \mathcal{O}(x^{-4})] & x \ll -1 \\ (2\pi x^2)^{-1/2} \exp(-x^2/2) [1 - x^{-2} + \mathcal{O}(x^{-4})] & x \gg +1 \end{cases}, \quad (\text{D32})$$

we can then write the argument of the logarithm in the definition of ψ to leading order in ε as

$$\begin{aligned} & \int_{-\infty}^{-Q} d\gamma(z_1) \left[1 - \frac{1}{\sqrt{2\pi}} \frac{\sqrt{\beta\varepsilon^{\ell/2}}}{\kappa + \sqrt{\tilde{q}_0} z_0 + \sqrt{\sigma^2 - \tilde{q}_0} z_1} \exp \left(-\frac{(\kappa + \sqrt{\tilde{q}_0} z_0 + \sqrt{\sigma^2 - \tilde{q}_0} z_1)^2}{2\beta\varepsilon^\ell} \right) \right]^{r\varepsilon} \\ & + \int_{-Q}^{\infty} d\gamma(z_1) \left[\frac{1}{\sqrt{2\pi}} \frac{\sqrt{\beta\varepsilon^{\ell/2}}}{\kappa + \sqrt{\tilde{q}_0} z_0 + \sqrt{\sigma^2 - \tilde{q}_0} z_1} \exp \left(-\frac{(\kappa + \sqrt{\tilde{q}_0} z_0 + \sqrt{\sigma^2 - \tilde{q}_0} z_1)^2}{2\beta\varepsilon^\ell} \right) \right]^{r\varepsilon}, \end{aligned} \quad (\text{D33})$$

where we have defined the function

$$Q \equiv \frac{\kappa + \sqrt{\tilde{q}_0} z_0}{\sqrt{\sigma^2 - \tilde{q}_0}} \quad (\text{D34})$$

for brevity. Using the continuity of the logarithm and passing to the limit $\varepsilon \downarrow 0$, this simplifies to

$$\int_{-\infty}^{-Q} d\gamma(z_1) + \int_{-Q}^{\infty} d\gamma(z_1) \lim_{\varepsilon \downarrow 0} \exp \left(-\frac{r(\kappa + \sqrt{\tilde{q}_0} z_0 + \sqrt{\sigma^2 - \tilde{q}_0} z_1)^2}{2\beta} \varepsilon^{1-\ell} \right) \quad (\text{D35})$$

for any $\ell > 0$. If $\ell < 1$, the remaining limit tends to unity, hence the argument of the logarithm tends to unity and ψ vanishes, resulting in a divergent 1-RSB capacity. If $g \in \mathcal{H}^1(\gamma)$, we have $\ell \geq 1$ and $\beta = \|g'\|_\gamma^2$, hence the 1-RSB capacity, like the RS capacity, remains finite. For functions of this class, evaluating the integrals over z_1 , we find that

$$\psi(q_0, r; \kappa) = - \int d\gamma(z_0) \log \left[H(Q) + R \exp \left(-\frac{1}{2} \frac{r(\kappa + \sqrt{\tilde{q}_0} z_0)^2}{\|g'\|_\gamma^2 + r(\sigma^2 - \tilde{q}_0)} \right) H(-QR) \right], \quad (\text{D36})$$

where Q is given as above and we have defined

$$R \equiv \sqrt{\frac{\|g'\|_\gamma^2}{\|g'\|_\gamma^2 + r(\sigma^2 - \tilde{q}_0)}} \quad (\text{D37})$$

for brevity.

Thus, the 1-RSB ansatz yields the same conditions on the activation function as the RS ansatz for the capacity to remain finite in the infinite-width. For a given activation function, we can in principle determine $\alpha_{1\text{-RSB}}$ numerically by solving an explicit two-dimensional minimization problem over $q_0 \in [0, 1]$ and $r_0 \in [0, \infty)$, though we do not obtain a simple closed-form solution like that for α_{RS} . We observe that the first-order conditions on q_0 and r resulting from this minimization are precisely the saddle-point equations for those order parameters. Unlike in the calculation of the RS capacity, we cannot in this case avoid the need to compute the effective order parameter $\tilde{q}_0(q_0)$ for generic values of q_0 . Finally, we note that expression for the 1-RSB capacity with $g(x) = \text{ReLU}(x)$ from [9] is equivalent in functional form to that presented here.

Appendix E: Calculation of the capacity for common activation functions

In this appendix, we provide details of the calculation of the RS and 1-RSB capacities for several commonly-used activation functions. Numerical computation of the 1-RSB capacity was performed in MATLAB 9.6. Integrals with respect to Gaussian measure were estimated using 20-point Gauss-Hermite quadrature [26], and minimization was performed using the interior-point solver `fmincon` [27]. These results were then checked against computations performed in MATHEMATICA 12.1 using the numerical integrator `NIntegrate` and minimizer `NMinimize` with 100 digits of internal precision. These methods were also used to generate and cross-check the contour plots in Figure 2 of the main text.

1. The rectified linear unit

The rectified linear unit $\text{ReLU}(x) \equiv \max\{0, x\}$ is the most commonly-used activation function in modern machine learning applications [5, 8], and has weak derivative $\text{ReLU}'(x) = \Theta(x)$. With our conventions, the Hermite expansion of ReLU is given as

$$\text{ReLU}(x) = \frac{1}{\sqrt{2\pi}} + \frac{1}{2} \text{He}_1(x) + \frac{1}{\sqrt{2\pi}} \sum_{k=1}^{\infty} \frac{(-1)^{k+1}}{2^k (2k-1)k!} \sqrt{(2k)!} \text{He}_{2k}(x). \quad (\text{E1})$$

By direct computation of the required integrals, we have

$$\sigma^2 = \frac{1}{2} - \frac{1}{2\pi} = \frac{\pi - 1}{2\pi} \quad (\text{E2})$$

and

$$\|\text{ReLU}'\|_\gamma^2 = \|\Theta\|_2^2 = H(0) = \frac{1}{2}, \quad (\text{E3})$$

hence we recover the result of Baldassi *et al.* [9] that

$$\alpha_{\text{RS}}(\kappa = 0) = \frac{2\pi}{\pi - 1} \simeq 2.93388. \quad (\text{E4})$$

For ReLU, we can express $\tilde{q}(q)$ in closed form by direct integration or by summation of the series expansion resulting from the function's Hermite expansion as

$$\tilde{q}(q) = \frac{q}{4} + \frac{q \arcsin(q) + \sqrt{1 - q^2} - 1}{2\pi}. \quad (\text{E5})$$

Using this formula, we obtain the estimate

$$\alpha_{1\text{-RSB}}(\kappa = 0) \simeq 2.66428 \quad (\text{E6})$$

at $(q_0^*, r^*) \simeq (0.75716, 16.63737)$.

This estimate of the 1-RSB capacity of a network with ReLU activations is lower than the $\alpha_{1\text{-RSB}} \simeq 2.92$ reported by Baldassi *et al.* [9]. This discrepancy likely results from the fact that they appear to have solved the saddle-point equations for q_0 and r numerically rather than directly minimizing over $\alpha_{1\text{-RSB}}$. Though these approaches are equivalent at the level of first-order conditions, it is possible that they yield different results when implemented numerically.

2. The Gauss error function

The Gauss error function

$$\text{erf}(z) = \frac{2}{\sqrt{\pi}} \int_0^z dx \exp(-x^2) = 1 - 2H(\sqrt{2}z) \quad (\text{E7})$$

is the most analytically convenient of the commonly-used sigmoidal activation functions. It has the Hermite expansion

$$\text{erf}(x) = \frac{2}{\sqrt{3\pi}} \sum_{k=0}^{\infty} \frac{(-1)^k}{3^k (2k+1)k!} \sqrt{(2k+1)!} \text{He}_{2k+1}(x), \quad (\text{E8})$$

which allows us to easily obtain the closed-form expressions

$$\tilde{q}(q) = \frac{4}{3\pi} \sum_{k=0}^{\infty} \frac{(2k+1)!}{3^{2k} (k!)^2 (2k+1)^2} q^{2k+1} = \frac{2}{\pi} \arcsin\left(\frac{2}{3}q\right) \quad (\text{E9})$$

and

$$\sigma^2 = \tilde{q}(1) = \frac{2}{\pi} \arcsin\left(\frac{2}{3}\right). \quad (\text{E10})$$

Similarly, we can easily work out that

$$\|\text{erf}'\|_{\gamma}^2 = \frac{2}{\sqrt{\pi}} \int d\gamma(x) \exp(-x^2) = \frac{4}{\sqrt{5}\pi}. \quad (\text{E11})$$

This yields

$$\alpha_{\text{RS}}(\kappa = 0) = \frac{4}{\sqrt{5} \arcsin(2/3)} \simeq 2.45140 \quad (\text{E12})$$

and

$$\alpha_{1\text{-RSB}}(\kappa = 0) \simeq 2.37500, \quad (\text{E13})$$

with $(q_0^*, r^*) \simeq (0.75463, 7.75682)$.

3. The quadratic

In neuroscientific studies of two-layer network models, expansive activations such as a quadratic are sometimes considered [28]. With $g(x) = x^2$, we can trivially work out that $\tilde{q}(q) = 2q^2$, hence we have $\sigma^2 = 2$ and $\|g'\|_2^2 = \|2x\|_{\gamma}^2 = 4$. Thus, we find that

$$\alpha_{\text{RS}}(\kappa = 0) = 4 \quad (\text{E14})$$

and

$$\alpha_{1\text{-RSB}}(\kappa = 0) \simeq 3.37466, \quad (\text{E15})$$

with $(q_0^*, r^*) \simeq (0.28452, 6.39299)$.

4. The hyperbolic tangent and logistic

Though it is less analytically convenient than the error function, the hyperbolic tangent and logistic sigmoid $g(x) = (\tanh(x) + 1)/2$ are more commonly used in practical applications [5]. We can numerically evaluate the required integrals, yielding $\|\tanh\|_\gamma^2 \simeq 0.39429$ and $\|\tanh'\|_\gamma^2 \simeq 0.46440$ and the estimate

$$\alpha_{\text{RS}}(\kappa = 0) \simeq 2.35561. \quad (\text{E16})$$

As the RS capacity is scale- and shift-invariant, the RS capacity of the logistic function is the same as that of the hyperbolic tangent.

5. The ‘‘Swish’’ and ‘‘Mish’’ functions

Recent experimental works on deep neural networks have proposed various smooth, non-monotonic functions as alternatives to the rectifier unit. One proposal is the product of a logistic function and a linear function, termed ‘‘Swish’’ [7, 8]:

$$\text{swish}(x; \beta) = \frac{x}{1 + \exp(-\beta x)}, \quad (\text{E17})$$

where β is a positive parameter. Conventionally, β is either fixed to unity or treated as a trainable weight, and yields the limiting behavior $\lim_{\beta \downarrow 0} \text{swish}(x; \beta) = x$, $\lim_{\beta \rightarrow \infty} \text{swish}(x; \beta) = \text{ReLU}(x)$. We can see that α_{RS} is a monotone increasing function of β , which tends to the perceptron result $\alpha_{\text{RS}}(\kappa = 0) = 2$ as $\beta \downarrow 0$ and the ReLU result $\alpha_{\text{RS}}(\kappa = 0) = 2\pi/(\pi - 1)$ as $\beta \rightarrow \infty$. With $\beta = 1$, we have $\|\text{swish}(\cdot; 1)\|_\gamma^2 \simeq 0.31308$ and $\|\text{swish}'(\cdot; 1)\|_\gamma^2 \simeq 0.37948$, and the estimate

$$\alpha_{\text{RS}}(\kappa = 0) \simeq 2.42416. \quad (\text{E18})$$

Another alternative to ReLU is the ‘‘Mish’’ function, defined as [7]

$$\text{mish}(x) = x \tanh \log(1 + \exp(x)), \quad (\text{E19})$$

for which we have $\|\text{mish}\|_\gamma^2 \simeq 0.47908$ and $\|\text{mish}'\|_\gamma^2 \simeq 0.39455$, and the estimate

$$\alpha_{\text{RS}}(\kappa = 0) \simeq 2.42852. \quad (\text{E20})$$